RESEARCH ARTICLE

endo-Fullerene and Doped Diamond Nanocrystallite-Based Models of Qubits for Solid-State Quantum Computers

Seongjun Park,[a] Deepak Srivastava,[b,*] and Kyeongjae Cho[c]

[a] *Department of Chemical Engineering, Stanford University, Stanford, California 94305-5025, USA*
[b] *Computational Nanotechnology at CSC/NAS, NASA Ames Research Center, Moffett Field, California 94035-1000, USA*
[c] *Department of Mechanical Engineering, Stanford University, Stanford, California 94305-4040, USA*

Models of encapsulated nuclear spin $\frac{1}{2}$ ^{1}H and ^{31}P atoms in fullerene and diamond nanocrystallite, respectively, are proposed and examined with an *ab initio* local density functional method for possible applications as single quantum bits (qubits) in solid-state quantum computers. A ^{1}H atom encapsulated in a fully deuterated fullerene, $C_{20}D_{20}$, forms the first model system and *ab initio* calculation shows that the ^{1}H atom is stable in its atomic state at the center of the fullerene with a barrier of about 1 eV to escape. A ^{31}P atom positioned at the center of a diamond nanocrystallite is the second model system, and ^{31}P atom is found to be stable at the substitutional site relative to interstitial sites by 15 eV. Vacancy formation energy is 6 eV in diamond, so the substitutional ^{31}P atom will be stable against diffusion during the formation mechanisms within the nanocrystallite. The coupling between the nuclear spin and the weakly bound (valance) donor electron coupling in both systems is found to be suitable for single qubit applications, whereas the spatial distributions of (valance) donor electron wave functions are found to be preferentially spread along certain lattice directions, facilitating two or more qubit applications. The feasibility of the fabrication pathways for both model solid-state qubit systems within practical quantum computers is discussed within the context of our proposed solid-state qubits.

Keywords: *endo*-Fullerene, Doped diamond nanocrystallite, Solid-state quantum computers, Quantum bits

1. INTRODUCTION

Quantum computers promise to exceed the computational efficiency of present day classical computers because quantum algorithms allow the execution of certain tasks in much fewer numbers of steps. Ones and zeros (bits) of classical computers are replaced by quantum states of a two-level system–a qubit. Logical operations are performed on qubits and their measurement determines the result.[1] Interest in quantum computations has recently increased dramatically for two reasons. First, efficient quantum algorithms for prime factorization and exhaustive database searches have been developed.[2,3] Second, quantum error-correcting codes have been developed that allow the operation of a quantum computer with a certain degree of decoherence in the quantum state, i.e., the quantum states need not be as coherent as previously thought.[4] The main difficulty is in realizing two-level quantum systems on which measurements can be made and which must be isolated from the environment as well.

Of many suggested models, the quantum states of spin $\frac{1}{2}$ particles, such as nuclear spins, have been proposed as isolated two-level quantum systems. A nuclear spin resonance approach, through nuclear magnetic resonance (NMR) experiments on bulk liquids, allows quantum computations by circumventing the single-spin detection problem.[5,6] Quantum computations that involve a few (up to seven) qubits have been demonstrated so far, but the main problem is that NMR on bulk liquids may not be scalable to more than a few qubits system. As an alternative, following the same philosophy of treating nuclear spins as isolated two-level systems, a conceptual design for a solid-state quantum computer based on ^{31}P donor atom dopants in bulk silicon has been proposed by Kane.[7] The nuclear spin of a single ^{31}P donor atom in bulk silicon serves as a single qubit, and Kane has developed a scheme to control the state of the qubit through a coupling of the nuclear spin with the weakly bound donor electron of the dopant atom. The overall architecture involves making well-defined precise arrays of ^{31}P donor atoms in bulk silicon. The nuclear spin states of individual qubits and the interaction between the neighboring qubits are controlled

*Author to whom correspondence should be addressed.

  1533-4880/2001/01/1/7/$17.00+.25 doi:10.1166/jnn.2001.015

by electronic gates placed over each qubit and in the spacing between neighboring qubits. Four out of five valance electrons of a ^{31}P donor atom are used up in the tetrahedral covalent bonding with the silicon lattice, whereas the fifth donor electron exists in a weakly bound state with large spatial extension in the lattice. The external electronic gate over each qubit indirectly controls the nuclear spin state by manipulating the donor electron distribution, leading to a change in hyperfine interaction between the nuclear spin and the weakly bound donor electron. The electronic gates between two qubits similarly modify the overlap between the neighboring donor electron wave functions and control the interactions between the neighboring qubits.

The main requirements to realize Kane's architecture are the placement of ^{31}P dopant atoms in precise array locations, which are hundreds of nanometers beneath silicon surface layers, and the fabrication of electronic gates to control individual qubits and the interactions between them. There are major experimental challenges to realizing this architecture. The most critical is how to position dopant atoms at precise positions beneath the surface layers. Additionally, during fabrication steps, dopant atoms are very likely to diffuse away from initial positions due to thermal effects and, after fabrication, intrinsic defects (e.g., vacancies and self-interstitials) in silicon will induce additional transient enhanced diffusion (TED) of the dopant atoms. Kane himself noted these problems and predicted that the fabrication steps "will require significant advances in the rapidly moving field of nanotechnology."[7]

In this article, we report new model systems that can overcome the above-mentioned fabrication related difficulties. Based on *ab initio* feasibility simulations, in this work we propose and examine a possible solution that envisions using "encapsulated" nuclear spin $\frac{1}{2}$ donor atom dopants in fullerenes and diamond nanocrystallites as solid-state single qubits that could be used to realize a nuclear-spin-based architecture of solid-state quantum computers. Because nanocrystallite or fullerene encapsulated dopant atoms are larger than the single dopant atoms, they are easier to position and incorporate in precise locations. Furthermore, our calculations show that the dopant atoms are structurally much more stable against any diffusion both before and after fabrication. In the following text, we present details of the model systems for using encapsulated nuclear spin $\frac{1}{2}$ dopant atoms as solid-state quantum bits and discuss the possible fabrication pathways or steps that already have been demonstrated in experiments that are unrelated to quantum computers.

The main requirements for an encapsulated donor atom to serve as a solid-state qubit in any architecture for a quantum computer are the following. First, the donor atom must have a $\frac{1}{2}$ nuclear spin and an s-like donor electron with reasonable nuclear spin-electron coupling. Second, the donor electronic state must not be too tightly bound to the location of the atom. Third, the larger sized encapsulated donor atoms must be configurationally very stable against diffusion during and after fabrication. Additionally, fourth, we require that any proposed scheme have reasonably demonstrated experimental steps that contribute possible fabrication pathways. Based on these four requirements, in this work, we propose and examine two models of encapsulated nuclear spin $\frac{1}{2}$ atoms to serve as individual qubits in a solid-state quantum computer.[8–10] Coupling between neighboring qubits, either directly through diamond lattice or through any high K dielectric host lattice, is currently under investigation and will be described elsewhere.

The first model involves encapsulation of a nuclear spin $\frac{1}{2}$ ^{1}H atom in a fullerene, and the second model envisions encapsulation of a ^{31}P atom in a few nanometer sized diamond nanocrystallite to serve as single qubits. Arrays of such larger sized qubits are envisioned for future quantum computer applications.

2. MODEL 1. ^{1}H ATOM ENCAPSULATED IN A FULLERENE

To realize a nuclear-spin-based solid-state qubit, nuclear spin $\frac{1}{2}$ and strong nuclear spin-electron coupling are necessary conditions. One of the most promising candidates is atomic ^{1}H because it has nuclear spin $\frac{1}{2}$ (except in deuterium) and there is one valence electron in the s orbital that is tightly bound to the nuclear position with strong nuclear spin-electron coupling. However, the main challenge is that the atomic ^{1}H is very reactive and easily forms a covalent bond to become a molecular or chemisorbed species. The only available valance electron will be used up in the reaction making it unavailable for hyperfine contact coupling to the nuclear spin. Additionally, even if the ^{1}H atom can be kept in an atomic state, maintaining its position in a bulk lattice is very difficult because ^{1}H is a lightweight atom and is highly mobile even at very low temperatures. Therefore, a ^{1}H atom may not be suitable for a qubit application unless (a) it can be kept in its atomic state within a solid-state system and (b) its mobility is reduced significantly. Encapsulation of a ^{1}H atom within a fullerene may be a solution to satisfy the preceding conditions.

The internal chemical reactivity of fullerenes was first examined to verify if a ^{1}H atom can stay in an atomic state within a fullerene. The internal hydrogenation of a variety of fullerenes was examined with *ab initio* density functional theory (DFT) pseudopotential methods.[11] For this study, we examined two fullerenes, C_{36}[12] and C_{60},[13] and the main findings are as follows. There are several isomers for C_{36} and we have chosen to use C_{36} D_{6h}, which is known to be the most stable isomer.[12,14] The intrinsic structures of C_{36} and C_{60} were optimized using the DFT

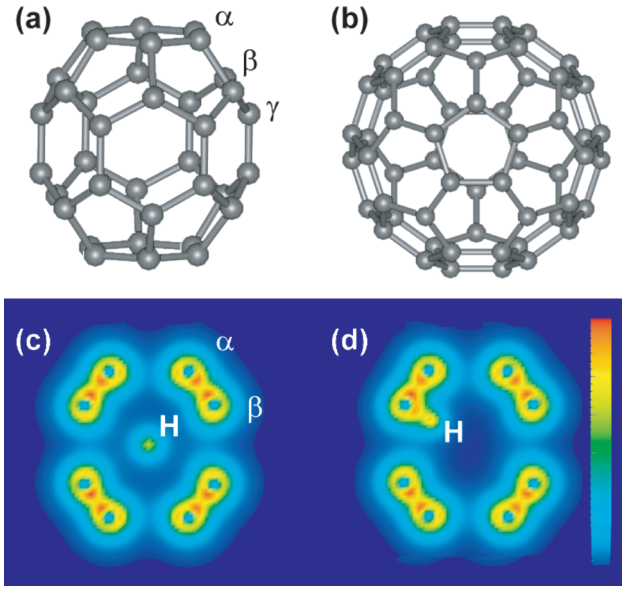

Fig. 1. (a) Atomic structure of the C_{36} molecule. Three different types of C atoms are labeled α, β, and γ. (b) Atomic structure of the C_{60} molecule. (c) Total valence electron density of $H@C_{36}$ with H at the center in the cross sectional plane containing the H atom, and α and β carbon atoms. (d) Valence electron density of $H@C_{36}$ with H bonded to a β carbon atom.

pseudopotential method,[11] and are shown in Figure 1a and b, respectively. C_{36} has three different types of C atom sites and C_{60} has one type of C atom site as indicated in the figure. All possible reactions of a ^{1}H atom with the internal binding sites of the fullerene-wall C atoms were examined, and the results are summarized in Table I.

When a ^{1}H atom is placed at the center of C_{36} or C_{60} fullerene, it has about –0.45 eV binding energy and the valance electron remains in its atomic state localized at the center. Figure 1c shows that the ^{1}H atom stays at the center of C_{36} and that the valance electron of the ^{1}H atom is well localized around the ^{1}H atom. Even though there are no significant bonds around the ^{1}H atom, the sum of small interactions (about –0.013 eV per C atom) between the ^{1}H atom and the surrounding 36 C atoms contributes toward a negative binding energy of –0.46 eV. However, the ^{1}H atom at the center is a metastable minimum energy configuration. In the global minimum energy configuration, the ^{1}H atom forms a covalent bond with the fullerene-wall carbon atom as shown in Figure 1d. The global minimum energy configuration at the fullerene-wall C atom is energetically more stable than the ^{1}H atom at the center by about 1 eV in both fullerenes. Similar results were found for other fullerenes studied.

Table I. Hydrogenation of C_{60} and C_{36}.

C_{36}				C_{60}	
Carbon A	Carbon B	Carbon C	Center	Carbon	Center
-1.28	-1.54	-1.40	-0.46	-1.23	-0.43

In general, the internal surfaces of fullerenes are relatively inert, and there are several successful examples of capturing an atom inside a fullerene without forming a covalent bond with a fullerene-wall C atom.[15,16] However, ^{1}H atoms are highly reactive, so the wall C atoms can form covalent bonds with encapsulated ^{1}H. Thus the encapsulated ^{1}H atom, if prepared, is most likely to react with the wall C atoms and will not have strong enough hyperfine contact coupling for qubit application. This situation can be reversed if the internal chemical reactivity of the fullerene-wall C atoms can be reduced. Because the internal and external reactivity of the fullerene-wall C atoms is due to π electron density, which has mixed hybridization (between sp^2 and sp^3) of the wall C atoms,[17] the internal reactivity could be reduced by removing the π electron density of the wall C atoms. In general, this can be achieved by hydrogenation of the exterior of the wall C atoms of the fullerene. External hydrogenation removes the most reactive π electron states from the interior, so that a ^{1}H atom can be stable at the center.

As an example, the encapsulation of a ^{1}H atom in a dodecahedrane $C_{20}H_{20}$, which is shown in Figure 2a, was investigated. The changes in the binding energy of a ^{1}H atom on the internal surface of $C_{20}H_{20}$ were calculated. The $C_{20}H_{20}$ hydrogenated fullerene has three high symmetry binding sites on the internal surface of the fullerene. The three sites are on top of the C atoms, on the center of the bonds between the C atoms, and on the center of C atom pentagon rings. Binding energies along all three sites were computed as a function of the distance from the center, and the results are shown in Figure 2b. Whereas all the C atoms are now fully saturated with four covalent bonds (of sp^3 type), there is no binding between the ^{1}H atom and internal surface of the fullerene. As a result, Figure 2b shows that the ^{1}H atom at the center site is the global minimum energy configuration and there is no metastable minimum energy configuration. The energetics of a possible diffusion path of the ^{1}H atom from the center of $C_{20}H_{20}$ to the center of a fullerene-wall pentagon shows that the barrier to escape from the fullerene is about 1 eV through the pentagons. This result is consistent with some other recent experimental[18] and theoretical[19] studies.

The spatial distribution of the valance electron of the ^{1}H atom encapsulated within $C_{20}H_{20}$ was also studied. This value is needed to estimate the coupling between neighboring qubits through valance electron overlaps of the neighboring qubits. If the valance electron wave function is totally trapped or shielded within the encapsulating fullerene ($C_{20}H_{20}$), the preceding model will not be useful for more than a single qubit system. Figure 2c shows that the valance electron density of the ^{1}H atom encapsulated within $C_{20}H_{20}$ is mostly concentrated at the center. Drawn at a different scale in Figure 2d, the valance electron density is shown to be leaking outside of the encapsulating fullerene, which indicates that the sp^3 bonded fullerene

RESEARCH ARTICLE

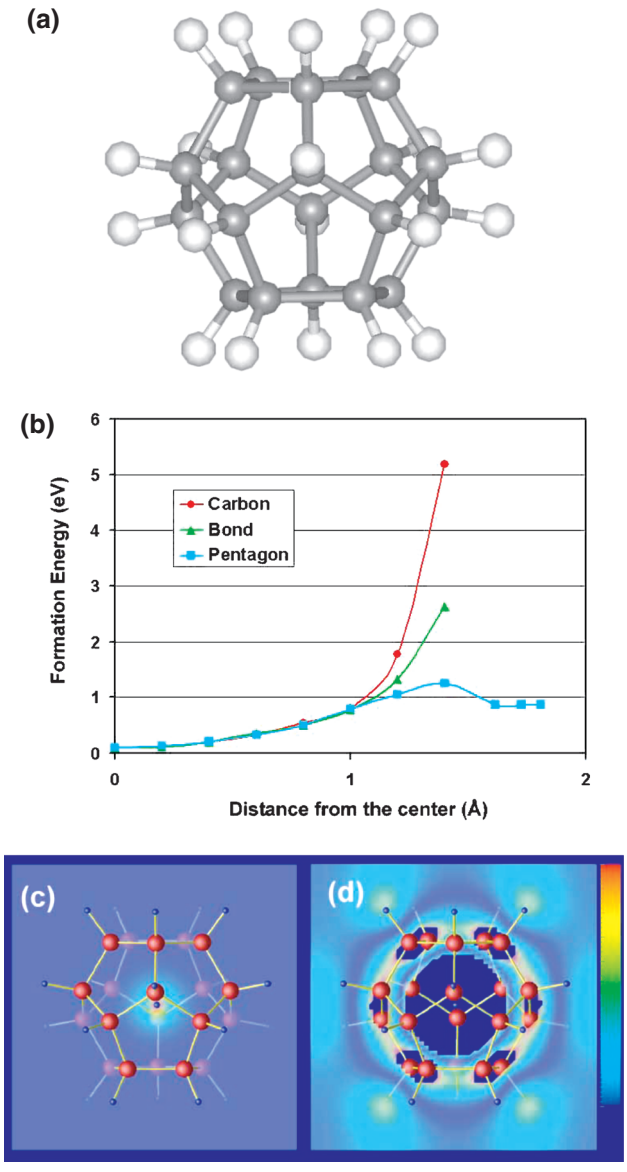

Fig. 2. (a) Atomic structure of the $C_{20}H_{20}$ molecule (dark gray balls = C and light gray balls = H). (b) Formation energy of $H@C_{20}H_{20}$ relative to an isolated H atom and a $C_{20}H_{20}$ molecule. The H atom has the lowest energy at the center of $C_{20}H_{20}$, and a 1.2 eV diffusion barrier of escaping through the center of a pentagon ring of $C_{20}H_{20}$. (c) Valence electron density of the H atom at $C_{20}H_{20}$, indicating a localized atomic state. (d) Valence electron density of (c) magnified 300 times with the central density (circular blue region) removed for the clarity of presentation. The $C_{20}H_{20}$ structure is shown to extend the atomic electron density beyond the encapsulating cage structure.

shell increased the range of electron distribution through a dielectric screening similar to a diamond lattice (ε = 5.5). The high valance electron density region at the center is removed and shown as a blank due to the scale of the electronic density plotted in Figure 2d. When the ^{1}H atoms on the outer surface of the $C_{20}H_{20}$ are replaced with deuterium (^{2}D) atoms, the valance electron density plots remain same as shown in Figure 2c and d. Additionally, the advantage is that the deuterium atoms have nuclear spin 1 with quite different resonance frequency from ^{1}H atoms [e.g., $\nu(^2D)$ = 6.5 MHz and $\nu(^1H)$ = 42.6 MHz for H_0 = 1 T] so that the possible interference of H atoms with $C_{20}H_{20}$ in nuclear spin measurements can be removed in this qubit Model 1 system (^1H @ $C_{20}D_{20}$).

3. MODEL 2. ^{31}P ATOM ENCAPSULATED IN A DIAMOND NANOCRYSTALLITE

A ^{31}P atom has nuclear spin $\frac{1}{2}$ and is the only natural isotope. When it is used as a dopant in any diamond lattice structured materials (e.g., group IV elements in the periodic table), its four valence electrons participate in tetrahedral covalent bonds. The fifth electron exists in a weakly bound s-like orbital within the lattice. Using this property, a conceptual design of a solid-state quantum computer based on arrays of ^{31}P atoms in bulk Si was proposed by Kane.[7] As discussed previously, the major obstacle to this proposal is the experimental difficulty in fabricating arrays of donor atom dopants, ^{31}P, beneath Si surface layers and the stability of dopant atoms. A possible solution to overcome these difficulties is to encapsulate the ^{31}P atom in a diamond nanocrystallite (2–10 nm sized) in a similar way as suggested for ^{31}P substitutional doping in bulk silicon, and then use the doped nanocrystallite as a single qubit. The main requirements for a ^{31}P doped diamond nanocrystallite to work as a single qubit are (a) a ^{31}P doped at a substitutional site in a diamond nanocrystallite must be a stable structure with minimal or no possibility of diffusion to the nanocrystallite surface, (b) a weakly bound donor electron in the lattice must be strongly coupled to nuclear spin through hyperfine contact interaction, (c) the donor electron wave function in the lattice must have sufficient spread to allow for coupling between neighboring qubits, and (d) fabrication pathways for ^{31}P doping in a diamond nanocrystallite must be experimentally feasible.

It turns out that the proposed model of ^{31}P doped in a diamond nanocrystallite can be fabricated through experimentally feasible steps as we suggested recently.[8–10] The steps are (1) encapsulate a ^{31}P atom at the center of a fullerene to make an *endo*-fullerene, $^{31}P@C_{60}$, (2) use the thus generated *endo*-fullerene to grow bucky onion (concentric graphitic spherical shells) layers on the *endo*-fullerene, (3) use electron-beam irradiation on the outer most bucky onion layers, followed by annealing of the system to convert the core layers into a diamond nanocrystallite with a ^{31}P atom trapped at the center, (4) chemically clean the remaining bucky onion layers to finally get a diamond nanocrystallite doped with a single ^{31}P donor atom at the center. The energetic, structural, and electronic behaviors of these processes involved in the preceding steps are examined via DFT pseudopotential methods.[11]

The first step in encapsulating a ^{31}P atom in a variety of fullerenes has been investigated for stability and positioning of the ^{31}P atom inside fullerenes. Whereas C_{60} is a seed material for bucky onion growth, we focus our discussion on the encapsulation of ^{31}P in a C_{60} fullerene. A ^{31}P atom was inserted within a fullerene and structural stability, binding sites, and electronic properties were investigated. Two energetically stable configurations are identified such that the ^{31}P atom either stays at the center of C_{60} or on top of a C—C bond that connect two pentagons on the wall of C_{60}. The binding energies are –0.99 and –0.81 eV for center site and on bond top site, respectively. Therefore, ^{31}P atom stays at the center of the fullerene. Recent experiments have put a ^{31}P atom into C_{60} using ion implantation.[16] Experimentally, ^{31}P was found to be most likely at the center of C_{60}. This is in agreement with our results based on the DFT pseudopotential method. The electron density of the donor electron in ^{31}P in C_{60}, shown in Figure 3a, exhibits a well-isolated ^{31}P atom at the center of the C_{60} fullerene; hence, the thus impregnated ^{31}P @ C_{60} fullerene is suitable as a seed material for growing bucky onion layers.

The step where core layers of a bucky onion are converted into diamond nanocrystallite at pressures above 20 GPa has already been demonstrated in experiments.[20,21] Conversion is done by inflicting electron-beam irradiation induced defects and etching into the outermost shells of the bucky onions. During the annealing process, defective outer shells with reduced numbers of C atoms form smaller radii and, consequently, exert an inward hydrostatic compression, as much as 50–150 GPa, on the inner core shell layers. At such high pressures, graphitic to diamond structural transition occurs, creating a diamond nanocrystallite of 2–50 nm diameter.[21] Furthermore, experiments have found single crystal diamond formation in smaller sized (2–10 nm) crystallites, and polycrystalline diamond formation in larger sized crystallites. Through DFT pseudopotential calculations, we have examined the structural and electronic properties of the ^{31}P atom substituted in a regular and compressed diamond nanocrystallite.

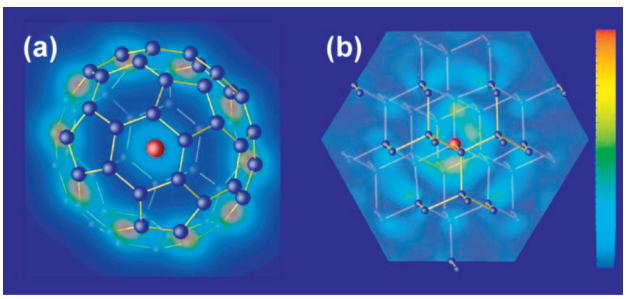

Fig. 3. (a) Total valence electron density of ^{31}P at the center of C_{60} fullerene in a cross sectional plane containing the P atom. (b) Donor electron density of ^{31}P in a diamond nanocrystallite shown in a (111) plane containing the P atom.

To gauge the most likely configuration of the ^{31}P atom during the nanocrystallite formation process, we examined the formation energy and structural configuration of ^{31}P doped in a diamond nanocrystallite for the three most possible configurations with ^{31}P at a substitutional site and ^{31}P at hexagonal or tetrahedral interstitial sites. The hydrostatic pressure on the diamond nanocrystallite was varied from 0 to 50 GPa to simulate appropriate scaling down of the diamond lattice parameters during high pressure processing. The main results are summarized in Table II. As the pressure increases, the formation energies of all the ^{31}P doped configurations increase. This is natural because the ^{31}P atom is larger than the lattice C atom and there is increasingly less space for the ^{31}P in the lattice as pressure increases. Results in Table II show that the ^{31}P at the substitutional site is the most stable configuration, even in the highly compressed diamond lattices. The energy required to hop from a substitutional site to a hexagonal or tetrahedral interstitial sites is also much higher than the corresponding energy for a ^{31}P atom in a silicon lattice. This means that even though a ^{31}P at the substitutional site of a diamond lattice has a small positive formation energy (0.88 eV) relative to the phase separated diamond and bulk ^{31}P, the ^{31}P atom, once substituted via our proposed trapping mechanism, stays put because of very large energy barriers to diffusion out of the nanocrystallite.

The thermal stability of the ^{31}P atom at a substitution site configuration versus diffusion was tested by computing the vacancy and interstitial formation energies. Both of these intrinsic defects play key roles in the diffusion of atomic species in bulk semiconductor materials.[22] The results are summarized in Table II. The vacancy formation energy is fairly high (over 6 eV) and is not likely to be produced naturally during any process. The vacancy formation energy changes only very slightly as the pressure goes up. The self-interstitial formation energy is even higher than the vacancy formation energy due to the small atomic space in the diamond lattice. Table II also shows the formation energies of ^{31}P atom at interstitial sites, which can be formed by C self-interstitial defect and provide other important mechanisms of diffusion. The ^{31}P at a substitutional site of diamond is more favorable than any other interstitial site by over 15 eV, which provides a large amount of energy barrier against diffusion through a self-interstitial mediated kick-out mechanism. For comparison, the interstitial formation energy of a ^{31}P atom relative to a substitutional site is only around 3 eV in bulk

Table II. Formation energies.

	0 GPa	20 GPa	50 GPa	Si
Substitutional site	0.88	1.99	3.85	-5.75
Hexagonal site	15.95	18.26	21.99	-2.71
Tetrahedral site	19.13	21.53	25.35	-1.90
Vacancy	6.78	6.65	6.65	

silicon. In the Si lattice, both vacancy and self-interstitial defects have relatively low formation energy (3−4 eV), and both vacancy and interstitial mediated diffusion in Si are known to occur during the processing steps. This analysis shows that ^{31}P fabricated in diamond nanocrystallite-based arrays will be much more stable against any diffusion mediated disruption mechanism than ^{31}P atoms in silicon lattice.

Last, the donor electron density of the ^{31}P atom at the substitutional site within the diamond lattice is shown in Figure 3b. For brevity, we show the planar donor electron density profile in the (111) plane of the underlying diamond lattice structure. The electron density profile in the (111) plane is nearly symmetric and does not decay exponentially as expected for an isolated donor electron atom. Moreover, we found that the decay profile of the donor electron density within a diamond lattice structure is anisotropic and channeled favorably along certain lattice directions and not as favorably along other lattice directions. A detailed analysis of this property to facilitate interqubit coupling is currently underway and will be published elsewhere.

For a single qubit model, in this work, the only possible difference comes from changing the host material from bulk Si to diamond. The dielectric constant of diamond (ε = 5.5) is half that of bulk Si (ε = 11.7) and the effective mass of electrons in diamond is on the same order as that in bulk Si ($m_{\text{eff}}/m = 0.2$). Therefore, we estimate that the hyperfine coupling ($A \propto \varepsilon^{-3}$) needed to control a nuclear spin on a single qubit, through an electric field applied by an external gate, is about 8 times stronger in our model than in Kane's silicon-based model. This means that we could, in principle, use a weaker electric field than the field required in Kane's model for the same level of control and that the interqubit exchange frequency ($\nu \propto A^2$) will increase by 2 orders of magnitude. On the other hand, donor electron density overlap between neighboring qubits in bulk diamond reduces by a factor of 2 compared to that in bulk silicon ($a_B \propto \varepsilon$). The neighboring qubit interactions in our case thus would be weaker by the same factor as compared to the interactions proposed in Kane's model. This shows that the above-proposed model for a single qubit is well within the range of operating conditions elucidated by Kane. Detailed analyses that involve more than single qubit structures are currently underway and will be published elsewhere.

4. COMMENTS

In summary, two models that use the nuclear spin states of encapsulated atoms in fullerenes and diamond nanocrystallite are proposed and examined through *ab initio* DFT pseudopotential methods. The first model shows that a nuclear spin $\frac{1}{2}$ ^{1}H atom remains stable at the center of a $C_{20}D_{20}$ (deuterated) fullerene with a barrier of about 1 eV for the encapsulated ^{1}H atom to diffuse out of the qubit unit. In the second model, the formation energy of a ^{31}P atom at the substitutional site in a diamond nanocrystallite is found to be significantly less than the formation energies of vacancy (by 6 eV) and ^{31}P at interstitial (by 15 eV) sites. This proves that a ^{31}P atom substituted within a diamond nanocrystallite is much more stable than the similar substitution in bulk Si. The strength of hyperfine contact coupling for controlling a qubit via an external electric field has increased in our model, whereas the electron–electron coupling that depends on the donor electron overlaps requires a shorter interqubit distance. The nature and spatial extension of the electronic wave functions in the two models are found to be satisfactory for single qubit application. Furthermore, detailed analysis of the donor electron density channeling through a diamond lattice structure, which is important for two or more than two qubit systems, is currently underway and will be published elsewhere. The experimental fabrication steps needed to fabricate single qubits have been elucidated, and we have confirmed that these experiments have been already been performed separately for different nanotechnology applications without any connection to quantum computing.

After this manuscript was submitted, we became aware (thanks to referee's comments) of a European collaborative research project, Quantum Information Processing Device using Doped Fullerene (QIPD-DF) that has a similar broad nature.[23] It is very encouraging that this project also aims to apply fullerene encapsulated atoms and clusters for novel quantum information device applications. We note that our original research proposal[8] was based on multishell fullerenes for solid-state quantum computer applications, whereas the QIPD-DF project involves eight partners with diverse quantum information device processing concepts. Recently, Si cage clusters also were shown to encapsulate metal atoms, and these caged clusters may form seed materials of novel nanodevice fabrication.[24] However, precise control of surrounding Si cluster structures would be a challenge to overcome before this approach becomes a practical alternative to *endo*-fullerene-based nanodevices.

Acknowledgments: This research was supported by the National Aeronautics and Space Administration (NASA) Ames Director's Discretionary Fund awards to D.S. (NASA Ames) and K.C. (Stanford). D.S. also was supported by NASA contract 704-40-32 to CSC. The DFT simulations were performed under the NPACI allocation SUA239 (Nanoscale Materials Simulations). We thank T.R. Govindan, Vadim Smylenski, and Dogan Timucin (all at NASA Ames) for significant discussion.

References and Notes

1. See, for example, a recent review by A. Steane, *Rep. Prog. Phys.* **B61**, 117 (1998).
2. A. Ekert and R. Jozsa, *Rev. Mod. Phys. B* **68**, 733 (1996).
3. L. K. Grover, *Phys. Rev. Lett.* **79**, 325 (1997).
4. J. Preskill, *Proc. R. Soc. London Ser. A* **454**, 385 (1998).
5. N. A. Gershenfeld and I. L. Chuang, *Science* **275**, 350 (1997).
6. I. L. Chung, L. M. K. Vandersypen, X. L. Zhou, D. W. Leung, and S. Lloyd, *Nature* **393**, 143 (1998).
7. B. E. Kane, *Nature* **393**, 133 (1998).
8. D. Srivastava, K. Cho, and T. R. Govindan, Simulation Based Prototyping of Solid-State Quantum Computers: A Pathway for Revolutionary Computing in the 21st Century, DDF Proposal, 1999.
9. S. Park, D. Srivastava, and K. Cho, unpublished manuscript.
10. S. Park, D. Srivastava, and K. Cho, unpublished manuscript, 2000.
11. For a review of DFT simulation method, see M. C. Payne, M. P. Teter, D. C. Allan, T. A. Arias, and J. D. Joannopoulos, *Rev. Mod. Phys.* **64,** 1045 (1992).
12. C. Piskoti, J. Yarger, and A. Zettl, *Nature* **393**, 771 (1998).
13. H. W. Kroto, J. R. Heath, S. C. O'Brien, R. F. Curl and R. E. Smalley, *Nature* **318**, 162 (1985).
14. J. C. Grossman, M. Côté, S. T. Louie, and M. L. Cohen, *Chem. Phys. Lett.* **284**, 344 (1998).
15. T. A. Murphy, T. Pawlik, A. Weidinger, M. Hohne, R. Alcala, and J. M. Spaeth, *Phys. Rev. Lett.* **77**, 1075 (1996).
16. C. Knapp, N. Weiden, K. Kass, K. P. Dinse, B. Pietzak, M. Waiblinger, and A. Weidinger, *Mol. Phys.* **95**, 999 (1998).
17. A. Hirsch, *Top. Curr. Chem.* **198**, 1 (1998).
18. R. J. Cross, M. Saunders, and H. Prinzbach, *Org. Lett.* **1**, 1479 (1999).
19. D. A. Dixon, D. Deerfield, and G. D. Graham, *Chem. Phys. Lett.* **78**, 161 (1981).
20. M. N. Regueiro, P. Monceau, and J. L. Hodeau, *Nature* **355**, 237 (1992).
21. F. Banhart and P. M. Ajayan, *Nature* **382**, 433 (1996).
22. P. M. Fahey, P. B. Griffin, and J. D. Plummer, *Rev. Mod. Phys.* **61**, 289 (1989).
23. The QIPD-DF project web site is http://planck.thphys.may.ie/QIPDDF/ .
24. H. Hiura, T. Miyazaki, and T. Kanayama, *Phys. Rev. Lett.* **86**, 1733 (2001).

Received: 16 February 2001; Revised & Accepted: 23 March 2001.